Published in final edited form as:
FEBS J. 2012 August ; 279(15): 2695–2713. doi:10.1111/j.1742-4658.2012.08652.x.

DOMINANT-NEGATIVE EFFECT OF TRUNCATED MANNOSE 6-PHOSPHATE/INSULIN-LIKE GROWTH FACTOR II RECEPTOR SPECIES IN CANCER*

Jodi L. Kreiling[2,*], **Michelle A. Montgomery**[1,*], **Joseph R. Wheeler**[1], **Jennifer L. Kopanic**[1], **Christopher M. Connelly**[1], **Megan E. Zavorka**[1], **Jenna L. Allison**[1], and **Richard G. MacDonald**[1,¶]

[1]Department of Biochemistry and Molecular Biology, University of Nebraska Medical Center, Omaha, Nebraska 68198-5870

[2]Department of Chemistry, University of Nebraska at Omaha, Omaha, Nebraska 68182-0109

SUMMARY

Oligomerization of the mannose 6-phosphate/insulin-like growth factor II receptor (M6P/IGF2R) is important for optimal ligand binding and internalization. M6P/IGF2R is a tumor suppressor gene that exhibits loss of heterozygosity and is mutated in several cancers. We tested the potential dominant-negative effects of two cancer-associated mutations that truncate the M6P/IGF2R in ectodomain repeats 9 and 14. Our hypothesis was that co-expression of the truncated receptors with wild-type/endogenous, full-length M6P/IGF2R would interfere with M6P/IGF2R function by heterodimer interference. Immunoprecipitation confirmed formation of heterodimeric complexes between full-length M6P/IGF2Rs and the truncated receptors, termed Rep9F and Rep14F. Remarkably, increasing expression of either Rep9F or Rep14F provoked decreased levels of full-length M6P/IGF2Rs in both cell lysates and plasma membranes, indicating a dominant-negative effect on receptor availability. Loss of full-length M6P/IGF2R was not due to increased proteasomal or lysosomal degradation, but instead arose from increased proteolytic cleavage of cell-surface M6P/IGF2Rs resulting in ectodomain release, by a mechanism that was inhibited by metal ion chelators. These data suggest that M6P/IGF2R truncation mutants may contribute to the cancer phenotype by decreasing availability of full-length M6P/IG2Rs to perform tumor-suppressive functions such as binding/internalization of receptor ligands like IGF-II.

Keywords

mannose 6-phosphate receptor; truncation mutants; dimerization; dominant negative; ectodomain shedding

INTRODUCTION

The mannose 6-phosphate/insulin-like growth factor II receptor (M6P/IGF2R) is a multifunctional transmembrane receptor of the p-lectin family that serves as both a tumor suppressor and in lysosome biogenesis [1, 2]. This 300-kDa glycoprotein has four major structural domains: the amino-terminal signal sequence, a short carboxyl-terminal cytoplasmic region, a single transmembrane domain, and a large extracytoplasmic region or

¶Please address correspondence to: Richard G. MacDonald, Ph.D. Department of Biochemistry and Molecular Biology, University of Nebraska Medical Center, 985870 Nebraska Medical Center, Omaha, NE 68198-5870, (402) 559-7824, Fax: (402) 559-6650, rgmacdon@unmc.edu.
*Indicates equal contribution to this body of work.

ectodomain. The ectodomain comprises 15 homologous repeating segments (termed mannose 6-phosphate receptor homology or MRH domains), each ~147 amino acid residues long and sharing 14–28% sequence identity [1, 3]. The M6P/IGF2R binds two major classes of ligand, M6P-bearing and non-M6P polypeptides, most of which bind to the receptor's ectodomain [3, 4]. Three M6P binding sites have been mapped to critical residues within repeats 3 and 9 (high affinity) and repeat 5 (low affinity) of the ectodomain [3]. Although these binding sites share the overall canonical fold of the MRH domains, each has distinctive binding properties, which manifest in differences in pH optima, preferences for binding M6P mono- vs. diester structures, and inter-repeat interactions required to form a functional binding site [2]. The M6P-bearing ligands include lysosomal acid hydrolases, transforming growth factor-β, proliferin, thyroglobulin, and granzyme B [2].

The non-M6P ligands of the M6P/IGF2R include the mitogen, insulin-like growth factor II (IGF-II), retinoic acid, and plasminogen. The binding site for IGF-II has been mapped to repeat 11 of the ectodomain, with structural stabilization of the binding region contributed by the 13th repeat [3]. Structural studies have shown that IGF-II binds within a hydrophobic pocket at the end of a β-barrel structure [5]. Binding of IGF-II plays an important role in the regulation of IGF-II action in target cells, leading to uptake into the cell and eventual degradation of IGF-II within lysosomes. This decrease in IGF-II availability reduces interaction of IGF-II with IGF-I receptors, contributing to the anti-proliferative and tumor-suppressive effects of the M6P/IGF2R [6–8]. Plasminogen binds to a site mapped to ectodomain repeat 1; this function of the M6P/IGF2R is thought to serve a role in mediating the proteolytic activation of plasminogen to plasmin [9].

Several groups have provided crystal structure data for portions of the M6P/IGF2R's ectodomain, allowing for insight into and model predictions of the overall structure of this large receptor [5, 10–12]. Structures of repeat 11, repeats 1–3, repeats 11–13, and 11–14 have been determined. The high level of sequence identity between the ectodomain repeats (14–28%) and/or between the repeats and the ectodomain of the cation-dependent M6P receptor (16–38%) accounts for structural similarities among the repeats, including conserved disulfide bond organization, and the overall flattened β-barrel structure of the repeats. The current model proposes that the M6P/IGF2R ectodomain is composed of tri-repeat units (repeats 1–3, 4–6, and 7–9) that stack on each other with a superhelical twist, with the distal six repeats of the ectodomain forming a larger hexameric unit (repeats 10–15) [5]. In this view, repeats 1–3 together form a high-affinity M6P-binding site, repeats 4–6 include a low-affinity M6P-binding site, repeats 7–9 encompass a second high-affinity M6P-binding site, and repeats 10–15 include the high-affinity IGF-II binding site and the region thought to stabilize dimer formation (repeat 12) [5, 13].

The M6P/IGF2R was long thought to function as a monomer; over the past decade, evidence has accumulated that indicates this receptor actually functions optimally as an oligomer in terms of high-affinity M6P-ligand binding and internalization of ligands. York *et al.* showed that binding of phosphomannosylated ligands with multiple M6P moieties, including β-glucuronidase, induced cell-surface oligomerization of the M6P/IGF2R resulting in more efficient uptake of receptor ligands by cross-bridging M6P/IGF2R molecules [14]. IGF-II binding did not appear to produce the same increase in receptor internalization, which is consistent with subsequent reports that IGF-II binds independently to both protomers of a dimeric receptor [17]. Byrd *et al.* further showed that dimer formation could occur regardless of the state of ligand binding for the receptor, likely mediated by interactions between repeats across receptor molecules [15, 16]. Mapping studies by Kreiling *et al.* determined that inter-subunit interactions appear to occur all along the M6P/IGF2R ectodomain, with particular stability of the dimer conferred by the presence of repeat 12

[13]. These data are supported by the composite model of the receptor assembled by Brown *et al.* [5].

Several studies have reported mutations in the *M6P/IGF2R* gene in various cancers that result in positioning a nonsense codon in-frame with prediction of premature termination, i.e., synthesis of receptors truncated within repeat 9 or repeat 14 of the ectodomain [17–19]. To date, there have been no functional studies of these truncated forms of the M6P/IGF2R; in particular, the possibility that they may form heterodimers with wild-type receptors and act in a dominant-negative manner has not been explored. In order to address how these mutations affect function of the wild-type receptors present in the same cells, we prepared mini-receptors that mimic these cancer-associated mutant receptor forms, termed Rep9F and Rep14F. Our hypothesis predicts that interaction of the full-length receptor with a truncated receptor in a heterodimeric structure would lead to interference with receptor functions, e.g., impaired IGF-II degradation and lysosomal enzyme sorting. Upon expression of these mutant constructs in HEK 293 cells, the truncated receptors were found both within the cells and secreted into the medium. The truncated receptors associated as dimers or in multimeric complexes with full-length endogenous M6P/IGF2R in cells. During experiments to test the possibility of dominant-negative effects on wild-type receptor, we observed marked loss of the endogenous receptors from the cells induced by expression of the truncated forms of the receptor. In this report, we provide evidence that the mechanism for this loss of M6P/IGF2R from cells expressing both the full-length receptor and a truncated form of the receptor is due to ectodomain shedding. We conclude that truncation mutants of *M6P/IGF2R* that occur in cancer cells may interfere with function of the normal gene product by dimerization leading to cleavage and enhanced rate of shedding of the imbalanced heterodimeric complex.

RESULTS

Transient expression of wild-type M6P/IGF2R with truncated receptors leads to destabilization of wild-type receptor expression

Several cancer-associated mutations of the *M6P/IGF2R* gene predict synthesis of truncated forms of the receptor. In one such case, mutations arise from microsatellite instability of a poly-G tract from nt 4089 to 4096; one- and two-base insertions in this tract were observed in gastrointestinal cancers [18] and squamous cell carcinoma of the lung [20]. The resultant frameshift brings a nonsense codon in-frame downstream of this site and causes premature termination of the protein. The deleted region encompasses part of repeat 9, all of repeats 10 through 15, the transmembrane region and the cytoplasmic domain, so there is potential for interference with both M6P- and IGF-II-binding functions. In another case, a C:G to A:T transversion observed in hepatocellular carcinoma at *M6P/IGF2R* nt 6410 creates an alternative splice site within intron 40 [17]. Abnormal splicing brings a nonsense codon in-frame immediately after Ser^{2023}, which produces a receptor truncated within repeat 14 that lacks repeat 15, the transmembrane and cytoplasmic domains.

In order to study the effects of the expression of truncated forms of M6P/IGF2R on the wild-type receptor's oligomeric structure and function, two truncation mutations bearing C-terminal FLAG tags, termed Rep9F and Rep14F, were designed and synthesized to mimic these naturally occurring receptor mutants (Fig. 1). In addition to the cancer-associated truncated constructs, a truncation construct containing the entire ectodomain region was evaluated (1–15F) in conjunction with the full-length, wild-type receptor construct containing a C-terminal Myc-epitope tag (WT-M). Ligand blotting experiments with lysates from cells transfected with each of the truncated receptor constructs were done to test for ligand binding properties (Fig. 1D). As predicted by its structure, Rep9F, which should contain only one intact binding site for M6P-based ligands, was not able to bind IGF-II, but

did bind the M6P pseudoglycoprotein ligand, pentamannosyl 6-phosphate-BSA (PMP-BSA). All of the other constructs (Rep14F, 1–15F, WT-M, and endogenous M6P/IGF2R) were able to bind both IGF-II and PMP-BSA (Fig. 1D), indicating that the truncated receptor proteins folded well enough to attain ligand binding function.

To test whether truncated receptor proteins could be expressed at detectable levels in cells, the Rep9F and Rep14F cDNA constructs were transiently expressed by co-transfection with WT-M cDNA into HEK 293 cells. Each truncated construct (Rep9F, Rep14F, or 1–15F) was transfected under a total of 8 conditions, in which the amount of cDNA for the truncated construct was increased and the amount of WT-M cDNA was held constant. The empty plasmid, pCMV5, was used as a negative control for expression of the tagged proteins (Fig. 2, *A–E, lane 1*). Whole-cell lysates were analyzed for relative expression levels of the receptors by immunoblotting with α-FLAG or α-Myc antibodies (Fig. 2, *A–C*).

Immunoblot analysis revealed that all of the truncated receptors were readily detectable in the 293 cells. However, in each series of transfections, the expression of WT-M decreased as a function of increasing input of 1–15F, Rep9F, or Rep14F cDNA, even though the input of WT-M cDNA was held constant at 5 μg in each condition tested (Fig. 2, panels A–C, *lanes* 2–7), suggesting that co-expression of the M6P/IGF2R constructs lacking the transmembrane and cytoplasmic domains somehow inhibited the expression of WT-M. Quantitative analysis of these data indicated that the effects of the Rep9F truncated receptor resulted in approximately 40–50% WT-M protein detected at the highest ratio of WT-M to Rep9F (4:1 Rep9F:WT-M) (Fig. 2C, *lane 7*). In contrast, Rep14F potently suppressed recovery of the WT-M protein to levels less than 10% of control at the highest transfection ratio (4:1 Rep14F/WT-M) (Fig. 2B, *lane 7*). Expression of the 1–15F truncated receptor also suppressed recovery of the WT-M protein (Fig. 2A, *lane 7*). These results indicate the possibility that formation of oligomeric complexes between full-length and truncated M6P/IGF2Rs destabilizes expression of the full-length receptor in HEK 293 cells.

To test whether this same phenomenon also affected the endogenous M6P/IGF2R, this experiment was repeated by transfecting HEK 293 cells with increasing concentrations of the truncated Rep9F and Rep14F constructs (Fig. 2, panels D and E). With increasing expression of Rep9F or Rep14F, the amount of endogenous M6P/IGF2R detected in the cell extracts decreased (Fig. 2D and 2E). These data suggest that transfection of these truncated M6P/IGF2Rs suppresses expression of the exogenous full-length WT-M as well as decreases measurable levels of the endogenous M6P/IGF2R within cells.

Truncated forms of the M6P/IGF2R dimerize with the full-length M6P/IGF2R

The suppressive effect of the truncated receptors on the full-length M6P/IGF2R could be mediated at the pre- or post-transcriptional levels. The latter possibility implies that the co-transfected truncated forms of the M6P/IGF2R can interact by dimerization with the full-length receptor. To test this hypothesis, HEK 293 cell lysates containing co-expressed FLAG and Myc epitope-tagged receptors were analyzed by an immunoprecipitation assay using α-FLAG affinity resin (Figs. 3 and 4). Analysis of the immunoblots revealed that essentially all of the expressed FLAG-tagged truncated receptors precipitated with the α-FLAG affinity resin (Figs. 3 and 4: *compare resin FLAG blot to direct-loaded lysate FLAG blot*). The data in Figures 3 and 4 indicate that the Myc-tagged full-length receptor did not immunoprecipitate in the absence of the FLAG-tagged truncated partner (Fig. 3 and 4, *lane 2*), but was detectable in the presence of FLAG-tagged truncated partners (Fig. 3 and 4, *lanes 3–7*). These data indicate that these differentially epitope-tagged M6P/IGF2Rs were capable of association as asymmetric oligomers.

In these experiments, co-transfection of either Rep9F (Fig. 3) or Rep14F (Fig. 4) at increasing ratios of truncated construct to full-length WT-M again suppressed the overall expression of the WT-M protein, as indicated by the progressive loss of detectable WT-M with expression of increasing amounts of truncated receptor. This loss of WT-M protein expression was again much more pronounced when co-expressed with the Rep14F truncated receptor, making it difficult to observe WT-M in co-immunoprecipitation experiments in which the precipitating antibody was anti-FLAG (Fig 4B). These data also indicate that these truncated M6P/IGF2R forms may indeed have dominant-negative effects on M6P/IGF2R availability when expressed from a mutant allele in cancer cells.

To ascertain that the observed interactions were not merely a result of the use of the αFLAG affinity resin, reciprocal immunoprecipitation experiments were also performed using theα-Myc antibody followed by precipitation with protein G-Sepharose. The data in Figures 3D and 4D indicate that WT-M was immunoadsorbed to the α-Myc matrix as expected. More importantly, when WT-M was used as the bait in co-immunoprecipitation, we observed that Rep9F (Fig. 3C, *lower panel*) and Rep14F (Fig. 4C, *lower panel*) were readily detected as interacting with WT-M.

One condition that must be fulfilled by the truncated receptors in order to affect M6P/IGF2R functions is that the dominant-negative effect on full-length M6P/IGF2R seen at the whole-cell level must be reflected in reduced receptor numbers at the cell surface. Thus, to provide a more direct test of this hypothesis, we measured the effect of expressing the truncated forms of the receptor on the amount of full-length M6P/IGF2R in plasma membranes of HEK 293 cells (Fig. 5). In this experiment, expression of Rep14F was not as high as seen in some of the earlier experiments—note that the Rep14F protein is readily detected in the anti-M6P/IGF2R blots, but not so well in the anti-FLAG blots. Nevertheless, expression of either truncated receptor decreased the amount of full-length receptors measured in lysates, either the endogenous M6P/IGF2R or the co-transfected WT-M protein (Fig. 5A). Importantly, this same effect was observed in plasma membranes prepared from cells in this same transfection experiment (Fig. 5B). Analysis of the band intensities on the anti-M6P/IGF2R blots from three experiments revealed that both Rep9F and Rep14F suppressed the level of full-length endogenous and WT-M receptors in cell lysates by 21–28%. In the plasma membranes, Rep9F was less potent than Rep14F in this regard, producing reductions of 13% and 30%, respectively. Only the effect of Rep14F on the amount of full-length receptor (endogenous M6P/IGF2R or WT-M) was significant, in both lysates and plasma membranes. Nevertheless, these data support the conclusion that the effect seen in whole-cell lysates was reflected in plasma membranes, i.e., the cell-surface receptor complement.

Presence of Rep9F or Rep14F does not alter the half-life of the wild-type M6P/IGF2R

To determine whether the apparent loss in expression of the full-length receptor induced by expression of the truncated M6P/IGF2Rs was due to an alteration in the receptor's degradative rate, we examined protein half-lives by metabolic labeling. Metabolic labeling experiments were carried out in HEK 293 cells transiently expressing WT-M alone or WT-M in combination with Rep9F or Rep14F. No significant overall differences were observed among the half-lives of WT-M in the presence or absence of Rep9F or Rep14F (data not shown). The half-life calculated for all receptor species was ~16 h, which agrees with published values [21, 22]. These experiments were also performed with varied chase times, from 6 to 12 h, and in the presence of cycloheximide to inhibit radiolabel reutilization via protein synthesis during the chase period (data not shown). These experiments resulted in the same calculated half-life of 16 h and no observed differences among the different receptor species.

Dimer interference effects of the Rep9F and Rep14F truncated M6P/IGF2Rs are not due to receptor degradation by the lysosomal or proteasomal pathways

In order to further investigate the mechanism of the loss of WT-M expression when there is an increase in expression of truncated M6P/IGF2Rs, we determined if the presence of the truncated receptor in complex with full-length receptors triggered some form of targeted degradation of the asymmetric heterodimeric complexes by either the proteasomal or lysosomal degradative pathways.

The involvement of lysosomes in the decreased protein expression of wild-type M6P/IGF2R was first examined by exposing HEK 293 cells that had been transfected with the various truncated and full-length M6P/IGF2R constructs to either 0, 100, or 200 μM chloroquine for 16 h (Fig. 6). Chloroquine is a lysosomotropic agent that accumulates in the lysosomes causing an alkalinization of the lysosomal lumen and thereby inhibiting activity of acid hydrolases within the organelle [23]. After treatment with chloroquine, the expression of each receptor construct was analyzed by immunoblotting with α-FLAG or α-Myc antibodies (Fig. 6). Chloroquine-induced inhibition of lysosomal degradative processes had no apparent effect of the amounts of truncated or full-length receptors recovered in cell lysates, indicating that the wild-type M6P/IGF2R was not being trapped in the lysosome by the presence of the truncated receptors (Fig. 6A & B, compare amount of WT-M protein expressed in presence of 0–200 μM chloroquine for *conditions 3–4*). As a positive control for lysosomal degradation, the levels of cathepsin D were assessed. As expected, treatment with chloroquine increased the amount of immunodetectable cathepsin D in HEK 293 cell lysates during this same time period (Fig. 6C).

The effect of the 26S proteasomal inhibitor lactacystin [24] was next examined. Cells expressing WT-M, Rep9F, and/or Rep14F individually or in combination were treated with 0, 10, or 20 μM lactacystin for 16 h (Fig. 7). After treatment with lactacystin, cell extracts were analyzed by immunoblotting for the expression of each M6P/IGF2R construct (Fig. 7). The amounts of each form of the receptor present again were not altered by proteasomal inhibition, indicating that the wild-type receptor is not being degraded by this mechanism when truncated receptors are present (Fig. 7A & B, compare amount of WT-M protein expressed in presence of 0–20 μM lactacystin for *conditions 3–4*). As a positive control to establish that lactacystin did inhibit proteasomal degradation under these conditions, the levels of c-Myc were assessed. As expected, treatment with lactacystin increased the levels of c-Myc in HEK 293 cell lysates (Fig. 7C).

Release of cell-surface M6P/IGF2Rs into the extracellular medium upon expression of truncated receptors

Proteolytic shedding of the ectodomain of membrane-bound receptors is an evolutionarily conserved post-translational modification by which transmembrane proteins are converted into soluble forms. A soluble, C-terminally truncated form of the M6P/IGF2R has been reported in the serum of several mammalian species [25–28]. This form of the receptor is ~20–30 kDa smaller than the intact membrane receptor and has been shown to lack the cytoplasmic and transmembrane domains [27]. Clairmont *et al.* [28] found that release of the soluble form of the M6P/IGF2R from cells can be blocked by the addition of serine protease inhibitors, indicating a proteolytic cleavage event, most likely at the cell surface, followed by release into the medium [28]. To test the possibility that this or a similar mechanism may underlie the dimer interference effects of the Rep9F and Rep14F truncated receptors on the WT-M receptor, we analyzed the expression of M6P/IGF2Rs in cell lysates *vs.* concentrated conditioned medium (CCM) after transfection with truncated receptors (Fig. 8).

The data in Figure 8 show that the amount of full-length endogenous receptor detected in lysates decreased somewhat as a function of increasing expression of Rep9F (Fig. 8A, upper band), but that expression of Rep14F had little detectable effect on the amount of endogenous M6P/IGF2R in these blots (Fig. 8B). These data contrast with the dramatic effect of truncated receptor expression on the exogenous full-length receptor (WT-M) (compare with the data in Fig. 2). This difference may be attributed to level of expression of the truncated receptors in the experiments shown in Figure 8, in better proportion to the amount of endogenous receptor in these cells (note that the bands in Figs. 8A and 8B were detected by the same antibody, α-M6P/IGF2R, rather than by an antibody against the epitope tag). Nevertheless, we detected large changes in the amounts of a form of the endogenous receptor released into the medium in response to expression of both truncated receptors (Fig. 8C and 8D).

In negative controls expressing no Rep9F or Rep14F, the amount of endogenous M6P/IGF2R found in the CCM is fairly low (Fig. 8; 0 μg lane). As the amount of Rep9F or Rep14F cDNA expressed in the cells increased, several changes were noted in the patterns of endogenous M6P/IGF2R species released. As a function of increasing expression of the Rep9F truncated receptor, we detected increased amounts of the endogenous M6P/IGF2R ectodomain in the CCM samples at the position on the blots corresponding to its calculated molecular weight of 250K (Fig. 8C; 2.5–20 μg lanes). However, a novel high-molecular-weight M6P/IGF2R species (HMW-M6P/IGF2R, indicated by the *asterisk* in Fig. 8C) also was detected in amounts that corresponded even more closely with the amount of transfected Rep9F. The HMW-M6P/IGF2R may reflect more dramatically the consequences of heterodimeric interactions between the endogenous receptor and this truncated species, leading to increased proteolytic cleavage of the full-length M6P/IGF2R and enhanced release into the extracellular medium. Similarly, expression of the Rep14F truncated receptor enhanced release both of the 250K M6P/IGF2R ectodomain (Fig. 8D) and of a novel HMW-M6P/IGF2R (Fig. 8D, *asterisk*). Determining the specific molecular weight of the HMW-M6P/IGF2R species was difficult because these gels were run under non-reducing conditions necessitated by the antibody. Comparison of the HMW-M6P/IGF2R species present in the Rep9F vs. Rep14F transfections indicates that these HMW species are of different weights consistent with the presence of the truncated Rep9F or Rep14F species in a putative complex. Based on molecular weight values of 145K for the Rep9F protein, 220K for Rep14F, and 250K for the cleaved M6P/IGF2R ectodomain, the migration behaviors of the HMW species are more consistent with a heterodimeric complex of Rep9F or Rep14F paired with the ectodomain of the endogenous M6P/IGF2R (Fig. 8C vs. 8D; note the spacing difference between endogenous (asterisk) and HMW (arrow) M6P/IGF2Rs in the Rep9F vs. Rep14F blots).

In contrast to a literature report [28], our laboratory, release of the M6P/IGF2R ectodomain into the medium was not inhibited by any of several serine protease inhibitors tested—phenylmethanesulfonyl fluoride (PMSF, 1 mM), aprotinin (50 mg/ml), or chymostatin (75 μM) (data not shown). Thus, we were unable to replicate the literature findings and began testing other agents known to block ectodomain release of various cell-surface receptors and cytokines through inhibition of matrix metalloproteinases (MMPs) or a disintegrin and metalloproteinase (ADAMs) [29, 30]. These enzymes require divalent cations for activity, more specifically, Zn^{2+}. We therefore tried several chelators as an initial, broad-based means of testing this notion. Direct incubation of cells for 48 hours with the chelating agents EGTA and EDTA produced some inhibition of ectodomain release (data not shown), but 1,10-phenanthroline (OPA), a chelator with strong, but not exclusive, affinity for Zn^{2+}, produced striking inhibition of M6P/IGF2R ectodomain release (Fig. 9). OPA at 1–5 mM concentrations had a pronounced sparing effect on the cellular levels of endogenous (Fig. 9A) and exogenous (WT-M, Fig. 9B) full-length receptors as well as both Rep9F and

Rep14F truncated species (Fig, 9, panels C and D, respectively). Conversely, release of all these forms of the receptor was inhibited under these conditions, suggesting a precursor-product relationship exists in which the soluble receptor in the medium arises from cleavage/release of the cellular M6P/IGF2R. Moreover, the protective effect of OPA on the Rep9F and Rep14F truncated forms suggests that at least some of them remain cell-associated through tethering by dimerization with full-length receptors. Overall, these data are consistent with the hypothesis that ectodomain release is mediated by a metalloproteinase, possibly one that is Zn^{2+}-dependent.

DISCUSSION

The original objective of this work was to investigate the implications of M6P/IGF2R dimerization to its function in the biology of IGF-II-stimulated cancers. The oligomeric nature of the M6P/IGF2R has been the subject of considerable investigation since Tong *et al.* reported that binding of monovalent phosphomannosyl ligands such as M6P to the bovine receptor was low-affinity while binding of bivalent ligands was high-affinity [31]. That work also revealed the stoichiometry of binding as two moles of M6P per mole receptor, suggesting a simple model of one bivalent ligand per receptor. Seminal work by York *et al.* [14] revealed that binding of a multivalent M6P-bearing glycoprotein such as β-glucuronidase (hGUS) promotes cross-bridging of two receptor molecules, and internalization of such ligand cross-bridged receptors occurred at a 3- to 4-fold faster rate than when bound to a ligand such as IGF-II that did not stabilize the dimeric structure [14]. Remarkably, M6P/IGF2R dimers cross-bridged by hGUS carried IGF-II into the cell at the accelerated rate [14]. Our laboratory has shown that M6P/IGF2R dimerization can occur in the absence of bound phosphomannosyl ligands [15, 16]. Dimer formation in this case appears to occur all along the ectodomains of neighboring monomers, with repeat 12 having a special stabilizing role [5, 13]. Thus, the current view is that the M6P/IGF2R exists as a dimer in the membrane and that binding of a bivalent phosphomannosyl ligand cross-bridges M6P binding sites on each monomer, stabilizing the dimeric structure and promoting a conformational change that facilitates endocytosis [32, 33].

Many cancers exhibit elevated levels of IGF-II expression that contribute to the growth factor-independent phenotype of the tumors [34]. Mitogenesis driven by IGF-II binding to the insulin-like growth factor I receptor or insulin receptor isoform A supports the rapid-proliferative phenotype of many types of cancer [1, 34]. In addition, the M6P/IGF2R may regulate proliferation and migration through its ability to bind and promote activation of plasminogen and transforming growth factor-β, as well as to maintain proper sorting of lysosomal enzymes [1,3,9]. The evidence for *M6P/IGF2R* as a tumor suppressor was developed initially for hepatocellular carcinoma through the work of Jirtle and colleagues [17, 35, 36] and has been the subject of several recent reviews [1, 12]. Evidence from transgenic animal work supports the hypothesis that the growth-suppressive effects of the M6P/IGF2R at the level of the whole animal derive mainly from the receptor's ability to bind pericellular IGF-II and to dispose of it by internalization and subsequent degradation [37, 38]. Overexpression of *M6p/Igf2r* inhibits tumorigenesis in a xenograft model using 66c14 mouse mammary tumor cells [8] and when mice slightly overexpressing *M6p/Igf2r* (~10% increase over control) are crossed with *Igf2* transgenic mice, tumor formation in the mammary glands of the offspring was significantly delayed [39]. *M6P/IGF2R* mutations of many types have been observed in HCC and colon carcinoma, including missense, frameshift and splicing mutations that result in synthesis of truncated proteins [17, 18, 20, 35]. The effects of several of these missense mutant forms of the receptor have been investigated in our laboratory [40, 41].

The dimeric structure of the M6P/IGF2R has implications for regulation of IGF-II-driven proliferation and survival in both normal and cancerous cells. There is now evidence that bivalent phosphomannosyl ligands can regulate cell proliferation by modulating availability of pericellular IGF-II. Cellular repressor of E1A-stimulated genes (CREG) is a phosphomannosylated lysosomal glycoprotein that is secreted by some cells [42]. Experiments in several cell lines indicate that secreted CREG can bind to the M6P/IGF2R and inhibit cell proliferation and migration by promoting receptor-mediated uptake and degradation of IGF-II [43–45]. However, there is still some uncertainty in this field, as a recent report indicated that CREG can bind to the repeats 11–13 region of the M6P/IGF2R in a manner that was independent of CREG glycosylation [46]. Our understanding of this phenomenon is too rudimentary to conclude that M6P-based ligands have a significant physiological role in regulating IGF-II availability in the homeostasis of normal tissues, but the possibility exists that abnormalities in the uptake and lysosomal degradation of IGF-II stimulated by multivalent phosphomannosyl ligands may contribute to the etiology of IGF-II-driven cancers.

Based on this rationale, we hypothesized that mutant M6P/IGF2Rs that interfere with the binding of M6P-based ligands or that create imbalanced receptor heterodimers may also contribute to cancer, either by reducing the level of functional M6P/IGF2R in cells, or in the context of biallelic *M6P/IGF2R* expression when one gene is wild type and the other mutant, a dominant-negative effect. Mutant M6P/IGF2Rs that seem most likely to produce such effects are truncation mutants of the receptor, of which two are known to occur in cancer. In the present study, we examined the effects of two cancer-associated mutations that are predicted to produce M6P/IGF2R species truncated in either the 9^{th} or 14^{th} ectodomain repeats [17, 18, 20]. Our finding that co-expression with a truncated receptor destabilizes the full-length or wild-type M6P/IGF2R implies that a tumor cell may enjoy the growth advantages of suppressed M6P/IGF2R activity despite the continued expression of wild-type receptor from one good allele, i.e., in the absence of loss of heterozygosity.

The novel observations of apparent instability of the full-length M6P/IGF2R when co-expressed with the cancer-associated truncated forms of receptor impelled us to revise our working hypothesis for how these mutant receptors may influence M6P/IGF2R actions in cells. Our focus shifted to examine the nature of the heterodimer interaction and to uncover the mechanism underlying this instability. Thus, in order to enable tracking of both the truncated and full-length receptor species, we engineered cDNA constructs encoding FLAG-tagged versions of the truncated Rep9 and Rep14 species and studied their effects in co-transfection experiments in HEK 293 cells with full-length, Myc-tagged M6P/IGF2R (WT-M). Our data clearly indicate that co-transfection of Rep9F or Rep14F with WT-M at increasing expression ratios suppressed expression of the WT-M receptor. The effect was more dramatic with Rep14F than with Rep9F, which may reflect that Rep14F was better able to form heterodimers with the full-length receptor. This may be due to the presence of Rep12 in the Rep14F truncated receptor, which may promote higher affinity dimerization with WT-M. Rep9F lacks this repeat, which has a prominent role in mediating intersubunit interactions of the dimeric M6P/IGF2R [5, 13]. Support for the hypothesis that this effect arose from formation of heterodimers between the truncated and full-length receptor species in cells was provided by co-immunoprecipitation experiments using detergent lysates of cells. It should be noted that these experiments have not directly shown that heterodimers can form within the membranes of intact cells. In addition, it was always much more difficult to demonstrate co-immunoprecipitation of Rep14F with WT-M, which we attribute to the high degree of instability in this heterodimeric species.

Importantly, transfection of either Rep9F or Rep14F on its own induced instability of the endogenous M6P/IGF2R, suggesting that this phenomenon is not simply an artifact of co-

transfection. Again, Rep14F was more potent in this regard than Rep9F. The data of York et al. [14] indicating that binding of multivalent phosphomannosyl ligands stabilizes the dimeric structure of the M6P/IGF2R raise another interesting question about the mechanism by which truncated receptors destabilize the wild-type receptor. Ironically, the binding of endogenous phosphomannosyl ligands may contribute to the destruction of the wild-type receptor by stabilizing heterodimers formed with truncated forms of the receptor. We plan to test this mechanistic possibility in future experiments through use of truncated receptors bearing mutations that knock out the main M6P binding sites in repeats 3 and 9.

To test the hypothesis that heterodimer instability was due to increased receptor degradation, we tested inhibitors of the major protein degradative pathways of the cell. However, chloroquine, an inhibitor of lysosome-mediated degradation, and lactacystin, an inhibitor of the proteasome pathway, had no effect on the receptor instability induced by the truncated M6P/IGF2R species. Comparisons of receptor degradative rates by metabolic labeling followed by immunoprecipitation also showed no effect. We concluded from these studies that if M6P/IGF2R loss was due to instability, that it did not involve any of the conventional pathways for protein breakdown, and that experimental approaches were needed to examine the products of the instability event rather than the intact receptors that remained.

Proteolytic shedding of the ectodomain of membrane-bound receptors is an evolutionarily conserved post-translational modification by which transmembrane proteins are converted into soluble forms. A soluble, C-terminally truncated form of the M6P/IGF2R lacking the cytoplasmic and transmembrane domains was discovered in the blood, amniotic fluid, and cerebrospinal fluid of several mammalian species [25–28]. Clairmont *et al.* [28] showed that release of the soluble form of the M6P/IGF2R from BRL-3A rat liver cells was blocked by the addition of the serine protease inhibitors aprotinin, chymostatin, and PMSF, indicating that the membrane-bound M6P/IGF2R undergoes proteolytic cleavage by a serine protease followed by release into the extracellular milieu. In our hands, these same serine protease inhibitors had no effect on the reduction in full-length cellular M6P/IGF2R or the increased release of the M6P/IGF2R ectodomain invoked by expression of the truncated receptors (data not shown). Furthermore, we found that metal ion chelating agents, particularly those that bind divalent cations such as Zn^{2+}, EDTA and OPA, not only blocked release of the M6P/IGF2R ectodomain under basal conditions, but also inhibited the increased release that occurred in the presence of the truncated receptors. Thus, we conclude that proteolytic release of the M6P/IGF2R ectodomain does not arise from cleavage by serine proteases, but instead, by one or more metalloproteinases. Furthermore, it appears that the receptor instability due to formation of imbalanced heterodimers between full-length and truncated receptor species increases the rate of release by this mechanism.

The phenomenon of proteolytic release of membrane proteins from the cell surface has been observed for many membrane proteins, including cytokines, growth factors, adhesion molecules and their receptors [29, 30]. In many cases, the enzymes implicated in these ectodomain shedding events are MMPs, zinc-containing endopeptidases that are involved in the metabolism of extracellular matrix [47]. MMPs are differentially sensitive to inhibition by divalent metal ion chelators. Some of the MMPs responsible for much of this sheddase activity are members of a disintegrin and metalloproteinase (ADAM) family of zinc (Zn) metalloproteinases [48–51]. The ADAMs are a large family of transmembrane and secreted proteins with functions in cell adhesion and proteolytic processing of the ectodomains of diverse cell-surface receptors and signaling molecules [51]. They contain a Zn binding site that is required for catalytic activity. ADAMs 9, 12, 15, and 17 stimulate proliferation of several cancer cell lines. While the current study was in progress, Leksa *et al.* [52] reported that release of the M6P/IGF2R ectodomain was mediated by ADAM17, and not ADAM10, in human umbilical vein endothelial cells. It is not known whether ADAM17-mediated

shedding of the M6P/IGF2R ectodomain is universal to all cells, but we are currently testing if this enzyme mediates the instability of imbalanced M6P/IGF2R heterodimers instigated by the cancer-associated truncation mutants as revealed in the present study. Nevertheless, the involvement of ADAM17 or potentially other metalloproteinases in this process provides further support for the important etiological role in cancer, including IGF-II-dependent cancers.

In summary, this study has revealed for the first time that M6P/IGF2R truncation mutants that occur in cancers have a dominant-negative effect on the overall expression of the receptor in cells, due to increased shedding of the receptor ectodomain. Our overall interpretation is that heterodimers of full-length receptor partnered with a truncated receptor may be more susceptible to cleavage or release from the cell surface. This may arise either from increased accessibility or steric facilitation of cleavage within the juxtamembrane region of the ectodomain of the full-length receptor, as well as the higher probability for release because a single cleavage event results in loss of tethering to the membrane rather than requiring two such cleavage events. Further work is needed to identify the metalloproteinase(s) involved and to establish the relevance of this phenomenon to specific cancers.

MATERIALS AND METHODS

Materials

Oligonucleotides were synthesized by Integrated DNA Technologies (Coralville, IA, USA). D-Mannose 6-phosphate (M6P) disodium salt, anti- (α)-FLAG M2 antibody, α-FLAG M2-agarose affinity gel, protein G-Sepharose, the protease inhibitor cocktail (PIC: aprotinin, [4-(2-aminoethyl)]benzenesulfonyl fluroride hydrochloride, bestatin hydrochloride, [N-(trans-epoxysuccinyl)-L-leucine] 4-guanidinobutylamide, leupeptin, and pepstatin A), cycloheximide, lactacystin, chloroquine, and the bicinchoninic acid kit for protein determination were purchased from Sigma (St. Louis, MO, USA). The α-Myc 9E10 antibody was purchased from Upstate Biotechnology, Inc. (Hercules, CA, USA), and the α-cathepsin D antibody was from R&D Systems (Minneapolis, MN, USA). The monoclonal anti-CD222 antibody MEM-238 (referred to as α-M6P/IGF2R throughout this report) was purchased from Abcam (Cambridge, MA, USA). Rabbit α-mouse IgG secondary antibody and the Amicon Ultra centrifugal filters were from Millipore (Billerica, MA, USA). Carrier-free $Na^{125}I$, ^{125}I-protein A, and the EasyTag™ EXPRE$^{35}S^{35}S$ protein labeling mix used for the pulse-chase experiments were from PerkinElmer Life Sciences (Waltham, MA, USA). Recombinant human IGFs were from Bachem (Torrance, CA, USA). Radiolabeled IGF-II and unlabeled and radiolabeled pentamannose phosphate-bovine serum albumin (PMP-BSA) were prepared as described previously [41]. The pCMV5 vector was provided by Dr. David W. Russell (University of Texas Southwestern Medical Center, Dallas, TX, USA) [53]. The 8.6-kilobase-pair human M6P/IGF2R cDNA was provided by Dr. William S. Sly (St. Louis University Medical Center, St. Louis, MO, USA) [54]. Other reagents and supplies were obtained from sources as indicated.

Preparation of Epitope-tagged Receptors

To study the effects of co-expressing cancer-associated truncated forms of the M6P/IGF2R with full-length receptor in cells, we designed two truncated mini-receptor constructs that mimic naturally occurring cancer-associated forms of the receptor (Fig. 1A) [17, 18]. The Rep9F construct encodes repeats 1 to 8 of the M6P/IGF2R ectodomain and a portion of repeat 9, ending after residue Thr^{1318} (Fig. 1B). The Rep14F construct encodes repeats 1 to 13 and a part of repeat 14, ending after Ser^{2023} (Fig. 1C). Both of these constructs include the signal sequence for proper sorting and localization within the cell [55] and each of the

mini-receptors bears a carboxyl-terminal eight-residue FLAG epitope tag (DYKDDDDK). To make the Rep9F construct, a cDNA fragment encompassing nt 94–4103 of the M6P/IGF2R cDNA was cloned into pCMV5RIX using High Fidelity PCR Supermix (Invitrogen), a 5′ primer targeted to nt 94–113 followed by an XhoI site, and a 3′-primer targeted to nt 4094–4103 followed by a FLAG-tag, stop codon, and an XbaI site. This construct was digested with EcoRI and XbaI and ligated into pCMV5RIX, generating the Rep9F construct (Fig. 1A). For the Rep14F construct, a cDNA fragment encompassing nt 94–6216 of the M6P/IGF2R cDNA, lacking nt 162–5319 that had been previously removed by EagI digestion, was cloned into pCMV5 with a 5′-primer targeted to nt 94–113 followed by a KpnI site, and a 3′-primer targeted to nt 6201–6216 followed by a FLAG-tag, two stop codons, and an XbaI site. This construct was digested with KpnI and XbaI and ligated into the pCMV5 vector. The mutant EagI fragment was then inserted into this intermediate construct, producing Rep14F (Fig. 1A). These constructs were designed to mimic the naturally occurring truncations as closely as possible with a FLAG epitope tag added for ease of purification and detection (Fig. 1B and C). Additionally, 1–15F and WT-M were used as controls in these experiments. The 1–15F construct encodes all 15 repeats of the M6P/IGF2R ectodomain followed by a FLAG epitope tag cloned into the pCMV5 vector as previously described (Fig. 1A)[15]. The WT-M construct encodes the full-length, wild-type receptor followed by a Myc epitope tag (MEQKLISEEDLN), subcloned into the target vector, pCMV5, in a multi-stage cloning procedure as previously described [13].

Transient Expression of Receptor Constructs

Human embryonic kidney (HEK) 293 cells were maintained in Dulbecco's modified Eagle medium (DMEM) supplemented with 7% fetal bovine serum (FBS) (Invitrogen/Life Technologies, Grand Island, NY, USA) and were grown at 37°C in a humidified atmosphere of 5% CO_2, 95% air. Transient expression of the various receptor constructs by calcium phosphate-mediated transfection into HEK 293 cells and immunoblot analysis of cell lysates to measure expression of the truncated and full-length receptors were performed as previously described [16, 56], except that the chloroquine shock was not performed. Whole-cell lysates were prepared from the 100-mm dishes on the third day following transfection with lysis extraction buffer (50 mM 4-(2-hydroxyethyl)piperazine-1-ethanesulfonic acid, pH 7.4, 1% Triton X-100 and 1 mM $MgCl_2$), as described previously [55]. Following incubation at 4°C, the suspension was centrifuged at 13,000 × g for 7 min and the supernatant was collected and stored at −80°C. Plasma membranes were prepared by Dounce homogenization and differential centrifugation as previously described [57]. Protein concentrations of lysates and plasma membrane suspensions were determined by the bicinchoninic acid assay. For transfections in which conditioned medium was collected, 24 h post-transfection the transfection medium was replaced with serum-free DMEM and allowed to incubate on the cells for 48 h. The conditioned medium (CM) was collected, supplemented with 1 mM PMSF and 1 mM sodium fluoride, and concentrated using an Amicon UltraR 10,000 molecular weight cutoff centrifugal filter by centrifuging the samples at 3,000 rpm for 15 min or until they were concentrated to ~1/20 volume. The protein concentration of the retentate was determined by the bicinchoninic acid assay and the concentrated conditioned medium (CCM) was stored at −20°C.

Analysis and Expression of M6P/IGF2R Constructs

Aliquots (20 μL or 100 μg of total protein as indicated) of Triton X-100 extracts or CCM were resolved by electrophoresis on reducing SDS-PAGE gels and transblotted to BA85 nitrocellulose paper (Schleicher and Schuell, Keene, NH, USA). The blots were incubated with blocking buffer (4% nonfat dry milk in 50 mM HEPES, pH 7.6, 150 mM NaCl, 0.1% Tween-20, 0.02% sodium azide) for 1 h at 22°C and probed with the appropriate antibody [α-M6P/IGF2R antibody (1:4000 dilution), α-FLAG antibody (1:1000), or α-Myc antibody

(1:500), all mixed as a solution with blocking buffer] for 1 h at 22°C. For the FLAG and Myc blots, a secondary antibody (rabbit α-mouse IgG, 1:1000 in blocking buffer) was then used for 30 min at 22°C. The blots were developed with ^{125}I-protein A (7 μCi in blocking buffer) for 30 min at 22°C, detected by autoradiography, and quantified using PhosphorImager analysis (Amersham Biosciences Corp., Piscataway, NJ, USA). Ligand blotting analysis with ^{125}I-IGF-II or ^{125}I-PMP-BSA was done according to previously published methods [58, 59].

Dimer Formation Assays

α-FLAG Immunoprecipitation—Aliquots (100 μg) of whole cell lysates prepared from HEK 293 cells co-transfected with the various cDNAs for the FLAG-tagged minireceptors and the Myc-tagged Man6P/IGF2R were incubated with 8 μL of packed M2 resin in HBS plus 1.0% BSA at 4°C for 3 h. The resin pellets were collected by centrifugation at 13,000 × *g* for 30 s and washed twice with 1 mL of HBS plus 0.05% Triton X-100 (HBST). Immunoblot analysis was performed by subjecting the resin pellets to treatment with sample buffer plus dithiothreitol, electrophoresis on 6% reducing SDS-PAGE gels, and transfer to BA85 nitrocellulose paper. The blots were probed with either α-FLAG or α-Myc monoclonal antibodies, incubated with secondary antibody, developed with ^{125}I-protein A, and detected by autoradiography. Levels of FLAG- and Myc-tagged proteins immunoprecipitated with the M2 resin were quantified using PhosphorImager analysis of the immunoblots. A second set of gels was run for each condition above containing an equal volume of lysate as a loading control.

α-Myc Immunoprecipitation—Aliquots of whole-cell lysates were incubated with 1 μL of α-Myc monoclonal antibody in HBST at 4°C for 16 h in a total reaction volume of 100 μL. Aliquots (25μl) of washed protein G-Sepharose resin slurry were added to the overnight incubations along with 75 μl of HBS plus 1.0% BSA + 5 mM M6P and then incubated at 4°C for 5 h. The resin pellets were collected by centrifugation and washed three times with 1 mL of HBST. Immunoblot analysis and quantification were performed as described above for the α-FLAG immunoprecipitation assays. A second set of gels was run as a loading control.

Pulse-Chase Experiments

HEK 293 cells were seeded at 6×10^6 cells per 150-mm dish, and the next day cells were singly- or co-transfected with WT-M, Rep9F, or Rep14F M6P/IGF2R constructs using calcium phosphate transfection. Prior to labeling, cells were grown to 90% confluence. Medium was then aspirated and replaced by serum-free DMEM lacking L-cystine and L-methionine (Invitrogen). To this was added 0.25 μCi/mL of ^{35}S-cysteine and ^{35}S-methionine using the EasyTag™ EXPRE^{35}S^{35}S protein labeling mix, 10 μM unlabeled L-methionine, and 0.4 mM L-glutamine (pulse medium). Cells were incubated for 30 min at 37°C, the pulse medium was removed, and the cell monolayers were quickly washed with 37°C serum-free DMEM containing 5 mM L-methionine (chase medium). After aspirating the wash medium, 10 mL of chase medium were added to the cells and incubated at 37°C for 0–6 h. At the indicated time points, the chase medium was removed and the cell monolayers were washed with 4°C phosphate-buffered saline (PBS). Whole-cell lysates were then subjected to α-Myc or α-FLAG immunoprecipitation and electrophoresed on a SDS-PAGE gel. The gels containing the ^{35}S-labeled proteins were stained with Coomassie brilliant blue, destained, dried, subjected to autoradiography and quantified using Typhoon PhosphorImager analysis.

Statistical Methods

Data sets in which the effect of increasing truncated receptor expression or inhibitor treatments was assessed on the amount of full-length receptor (i.e., Figures 2, 8, 9) were analyzed by regression analysis. Deviation of the slopes from zero was measured to test the null hypothesis. For experiments involving comparisons of different band intensities (absence (control) vs. presence of truncated receptor expression or +/− drug treatment groups, i.e., Figures 3, 4, 5) were calculated using a one-way analysis of variance (ANOVA) with Dunnett's test as a post-hoc analysis that compared specific group means (e.g., Rep9F and Rep14F) to a control group mean (pCMV5 vector control). Differences were considered significant at $P < 0.05$.

Acknowledgments

We are grateful to Scott Moon, Rachel Riebe, Aaron Pilley, Jennifer Bognich, and Philip Van DeVelde for their input and technical support. We thank Dr. William S. Sly for providing the human M6P/IGF2R cDNA and Dr. David W. Russell for providing pCMV5. We appreciate helpful discussion and suggestions from Dr. Richard Lomneth. This work has been supported by National Institutes of Health grant CA91885 and a grant from the Nebraska Department of Health and Human Services (to R.G.M.), the Nebraska EPSCoR Small Grant Program for Members of Underrepresented Groups in Science in Nebraska (to J.L.K.), and the University Committee on Research and Creative Activity and the College of Arts and Sciences at UNO (to J.L.K.). M.A.M. was the recipient of pre-doctoral stipend support provided by Graduate Studies and Skala Fellowships through the University of Nebraska Medical Center and fellowship from the Graduate Assistance in Area of National Need (GAANN) Program from the U.S. Department of Education. This project was supported by grants from the National Center for Research Resources (5P20RR018759-10) and the National Institute of General Medical Sciences (8 P20 GM103489-10) from the National Institutes of Health.

Abbreviations

M6P/IGF2R	mannose 6-phophate/insulin-like growth factor II receptor
MRH	mannose 6-phosphate receptor homology
IGF	insulin-like growth factor
WT-M	Myc-tagged wild-type M6P/IGF2R
M6P	mannose 6-phosphate
FBS	fetal bovine serum
HEK	human embryonic kidney
CM	conditioned medium
CCM	concentrated conditioned medium
OPA	1,10-orthophenanthroline
PBS	phosphate-buffered saline
PMSF	phenylmethanesulfonyl fluoride
PMP	pentamannosyl 6-phosphate
α-	anti-
CREG	cellular repressor of E1A-stimulated genes
HMW	high molecular weight
HER	human epidermal growth factor receptor
MMP	matrix metalloproteinase

ADAM a disintegrin and metalloproteinase

References

1. Martin-Kleiner I, Gall Troselj K. Mannose-6-phosphate/insulin-like growth factor 2 receptor (M6P/IGF2R) in carcinogenesis. Cancer Lett. 2010; 289:11–22. [PubMed: 19646808]
2. Dahms NM, Hancock MK. P-type lectins. Biochim Biophys Acta. 2002; 1572:317–340. [PubMed: 12223278]
3. Dahms NM. Insulin-like growth factor II/cation-independent mannose 6-phosphate receptor and lysosomal enzyme recognition. Biochem Soc Trans. 1996; 24:136–141. [PubMed: 8674625]
4. El-Shewy HM, Luttrell LM. Insulin-like growth factor-2/mannose-6 phosphate receptors. Vitam Horm. 2009; 80:667–697. [PubMed: 19251055]
5. Brown J, Delaine C, Zaccheo OJ, Siebold C, Gilbert RJ, van Boxel G, Denley A, Wallace JC, Hassan AB, Forbes BE, Jones EY. Structure and functional analysis of the IGF-II/IGF2R interaction. EMBO J. 2008; 27:265–276. [PubMed: 18046459]
6. O'Gorman DB, Costello M, Weiss J, Firth SM, Scott CD. Decreased insulin-like growth factor-II/mannose 6-phosphate receptor expression enhances tumorigenicity in JEG-3 cells. Cancer Res. 1999; 59:5692–5694. [PubMed: 10582686]
7. O'Gorman DB, Weiss J, Hettiaratchi A, Firth SM, Scott CD. Insulin-like growth factor-II/mannose 6-phosphate receptor overexpression reduces growth of choriocarcinoma cells *in vitro* and *in vivo*. Endocrinology. 2002; 143:4287–4294. [PubMed: 12399424]
8. Li J, Sahagian GG. Demonstration of tumor suppression by mannose 6-phosphate/insulin-like growth factor 2 receptor. Oncogene. 2004; 23:9359–9368. [PubMed: 15543235]
9. Leksa V, Godár S, Cebecauer M, Hilgert I, Breuss J, Weidle UH, Horejsí V, Binder BR, Stockinger H. The N terminus of mannose 6-phosphate/insulin-like growth factor 2 receptor in regulation of fibrinolysis and cell migration. J Biol Chem. 2002; 277:40575–40582. [PubMed: 12189157]
10. Olson LJ, Dahms NM, Kim J-JP. The N-terminal carbohydrate recognition site of the cation-independent mannose 6-phosphate receptor. J Biol Chem. 2004; 279:34000–34009. [PubMed: 15169779]
11. Olson LJ, Yammani RD, Dahms NM, Kim J-JP. Structure of uPAR, plasminogen, and sugar-binding sites of the 300 kDa mannose 6-phosphate receptor. EMBO J. 2004; 223:2019–2028. [PubMed: 15085180]
12. Brown J, Jones EY, Forbes BE. Keeping IGF-II under control: lessons from the IGF-II-IGF2R crystal structure. Trends Biochem Sci. 2009; 34:612–619. [PubMed: 19796953]
13. Kreiling JL, Byrd JC, MacDonald RG. Domain interactions of the insulin-like growth factor II/mannose 6-phosphate receptor. J Biol Chem. 2005; 280:21067–21077. [PubMed: 15799974]
14. York SJ, Arneson LS, Gregory WT, Dahms NM, Kornfeld S. The rate of internalization of the mannose 6-phosphate/insulin-like growth factor II receptor is enhanced by multivalent ligand binding. J Biol Chem. 1999; 274:1164–1171. [PubMed: 9873065]
15. Byrd JC, MacDonald RG. Mechanisms for high affinity mannose 6-phosphate ligand binding to the insulin-like growth factor II/mannose 6-phosphate receptor. Negative cooperativity and receptor oligomerization. J Biol Chem. 2000; 275:18638–18646. [PubMed: 10764735]
16. Byrd JC, Park JHY, Schaffer BS, Garmroudi F, MacDonald RG. Dimerization of the insulin-like growth factor II/mannose 6-phosphate receptor. J Biol Chem. 2000; 275:18647–18656. [PubMed: 10764761]
17. De Souza AT, Hankins GR, Washington MK, Orton TC, Jirtle RL. *M6P/IGF2R* gene is mutated in human hepatocellular carcinomas with loss of heterozygosity. Nat Genet. 1995; 11:447–449. [PubMed: 7493029]
18. Souza RF, Appel R, Yin J, Wang S, Smolinski KN, Abraham JM, Zou T-T, Shi Y-Q, Lei J, Cottrell J, Cymes K, Biden K, Simms L, Leggett B, Lynch PM, Frazier M, Powell SM, Harpaz N, Sugimura H, Young J, Meltzer SJ. Microsatellite instability in the insulin-like growth factor II receptor gene in gastrointestinal tumours [letter]. Nat Genet. 1996; 14:255–257. [PubMed: 8896552]

19. Ouyang H, Shiwaku HO, Hagiwara H, Miura K, Abe T, Kato Y, Ohtani H, Shiiba K, Souza RF, Meltzer SJ, Horii A. The insulin-like growth factor II receptor gene is mutated in genetically unstable cancers of the endometrium, stomach, and colorectum. Cancer Res. 1997; 57:1851–1854. [PubMed: 9157973]
20. Kong F-M, Anscher MS, Washington MK, Killian KJ, Jirtle RL. *M6P/IGF2R* is mutated in squamous cell carcinoma of the lung. Oncogene. 2000; 19:1572–1578. [PubMed: 10734317]
21. Sahagian GG. The mannose 6-phosphate receptor: function, biosynthesis and translocation. Biol Cell. 1984; 51:207–214. [PubMed: 6240303]
22. MacDonald RG, Czech MP. Biosynthesis and processing of the type II insulin-like growth factor receptor in H-35 hepatoma cells. J Biol Chem. 1985; 260:11357–11365. [PubMed: 2993308]
23. Blok J, Mulder-Stapel AA, Ginsel LA, Daems WT. The effect of chloroquine on lysosomal function and cell-coat glycoprotein transport in the absorptive cells of cultured human small-intestinal tissue. Cell Tissue Res. 1981; 218:227–251. [PubMed: 7261028]
24. Jockers R, Angers S, Da Silva S, Benaroch P, Strosberg AD, Bouvier M, Marullo S. Beta(2)-adrenergic receptor down-regulation. Evidence for a pathway that does not require endocytosis. J Biol Chem. 1999; 274:28900–28908. [PubMed: 10506134]
25. Kiess W, Greenstein LA, White RM, Lee L, Rechler MM, Nissley SP. Type II insulin-like growth factor receptor is present in rat serum. Proc Natl Acad Sci USA. 1987; 84:7720–7724. [PubMed: 2959961]
26. Causin C, Waheed A, Braulke T, Junghans U, Maly P, Humbel RE, von Figura K. Mannose 6-phosphate/insulin-like growth factor II-binding proteins in human serum and urine. Their relation to the mannose 6-phosphate/insulin-like growth factor II receptor. Biochem J. 1988; 252:795–799. [PubMed: 2458716]
27. MacDonald RG, Tepper MA, Clairmont KB, Perregaux SB, Czech MP. Serum form of the rat insulin-like growth factor II/mannose 6-phosphate receptor is truncated in the carboxyl-terminal domain. J Biol Chem. 1989; 264:3256–3261. [PubMed: 2536739]
28. Clairmont KB, Czech MP. Extracellular release as the major degradative pathway of the insulin-like growth factor II/mannose 6-phosphate receptor. J Biol Chem. 1991; 266:12131–12134. [PubMed: 1648081]
29. Black RA. Tumor necrosis factor-alpha converting enzyme. Int J Biochem Cell Biol. 2002; 34:1–5. [PubMed: 11733179]
30. Mullberg J, Althoff K, Jostock T, Rose-John S. The importance of shedding of membrane proteins for cytokine biology. Eur Cytokine Netw. 2000; 11:27–38. [PubMed: 10705296]
31. Tong PY, Gregory W, Kornfeld S. Ligand interactions of the cation-independent mannose 6-phosphate receptor. The stoichiometry of mannose 6-phosphate binding. J Biol Chem. 1989; 264:7962–7969. [PubMed: 2542254]
32. Ghosh P, Dahms NM, Kornfeld S. Mannose 6-phosphate receptors: new twists in the tale. Nat Rev Mol Cell Biol. 2003; 4:202–213. [PubMed: 12612639]
33. MacDonald RG, Byrd JC. The insulin-like growth factor II/mannose 6-phosphate receptor: implications for IGF action in breast cancer. Breast Disease. 2003; 17:61–72. [PubMed: 15687678]
34. Pollak MN, Schernhammer ES, Hankinson SE. Insulin-like growth factors and neoplasia. Nat Rev Cancer. 2004; 4:505–518. [PubMed: 15229476]
35. De Souza AT, Hankins GR, Washington MK, Fine RL, Orton TC, Jirtle RL. Frequent loss of heterozygosity on 6q at the mannose 6-phosphate/insulin-like growth factor II receptor locus in human hepatocellular tumors. Oncogene. 1995; 10:1725–1729. [PubMed: 7753549]
36. Hankins GR, De Souza AT, Bentley RC, Patel MR, Marks JR, Iglehart JD, Jirtle RL. M6P/IGF2 receptor: a candidate breast tumor suppressor gene. Oncogene. 1996; 12:2003–2009. [PubMed: 8649861]
37. Filson AJ, Louvi A, Efstratiadis A, Robertson EJ. Rescue of the T-associated maternal effect in mice carrying null mutations in *Igf-2* and *Igf2r*, two reciprocally imprinted genes. Development. 1993; 118:731–736. [PubMed: 8076514]

38. Ludwig T, Eggenschwiler J, Fisher P, D'Ercole AJ, Davenport ML, Efstratiadis A. Mouse mutants lacking the type 2 IGF receptor (IGF2R) are rescued from perinatal lethality in *Igf2* and *Igf1r* null backgrounds. Dev Biol. 1996; 177:517–535. [PubMed: 8806828]
39. Wise TL, Pravtcheva DD. Delayed onset of Igf2-induced mammary tumors in Igf2r transgenic mice. Cancer Res. 2006; 66:1327–1336. [PubMed: 16452186]
40. Devi GR, De Souza AT, Byrd JC, Jirtle RL, MacDonald RG. Altered ligand binding by insulin-like growth factor II/mannose 6-phosphate receptors bearing missense mutations in human cancers. Cancer Res. 1999; 59:4314–4319. [PubMed: 10485478]
41. Byrd JC, Devi GR, De Souza AT, Jirtle RL, MacDonald RG. Disruption of ligand binding to the insulin-like growth factor II/mannose 6-phosphate receptor by cancer-associated missense mutations. J Biol Chem. 1999; 274:24408–24416. [PubMed: 10446221]
42. Schähs P, Weidinger P, Probst OC, Svoboda B, Stadlmann J, Beug H, Waerner T, Mach L. Cellular repressor of E1A-stimulated genes is a bona fide lysosomal protein which undergoes proteolytic maturation during its biosynthesis. Exp Cell Res. 2008; 314:3036–3047. [PubMed: 18621046]
43. Di Bacco A, Gill G. The secreted glycoprotein CREG inhibits cell growth dependent on the mannose-6-phosphate/insulin-like growth factor II receptor. Oncogene. 2003; 22:5436–5445. [PubMed: 12934103]
44. Han Y, Cui J, Tao J, Guo L, Guo P, Sun M, Kang J, Zhang X, Yan C, Li S. CREG inhibits migration of human vascular smooth muscle cells by mediating IGF-II endocytosis. Exp Cell Res. 2009; 315:3301–3311. [PubMed: 19769965]
45. Han Y-L, Guo P, Sun M-Y, Guo L, Luan B, Kang J, Yan C-H, Li S-H. Secreted CREG inhibits cell proliferation mediated by mannose 6-phosphate/insulin-like growth factor II receptor in NIH3T3 fibroblasts. Genes Cells. 2008; 13:977–986. [PubMed: 18691225]
46. Han Y-L, Luan B, Sun M, Guo L, Guo P, Tao J, Deng J, Wu G, Liu S, Yan C, Li S. Glycosylation-independent binding to extracellular domains 11–13 of mannose-6-phosphate/insulin-like growth factor-2 receptor mediates the effects of soluble CREG on the phenotypic modulation of vascular smooth muscle cells. J Mol Cell Cardiol. 2011; 50:723–730. [PubMed: 21195083]
47. Seals DF, Courtneidge SA. The ADAMs family of metalloproteases: multidomain proteins with multiple functions. Genes Dev. 2003; 17:7–30. [PubMed: 12514095]
48. Arribas J, Massague J. Transforming growth factor-alpha and beta-amyloid precursor protein share a secretory mechanism. J Cell Biol. 1995; 128:433–441. [PubMed: 7844156]
49. Hundhausen C, Misztela D, Berkhout TA, Broadway N, Saftig P, Reiss K, Hartmann D, Fahrenholz F, Postina R, Matthews V, Kallen KJ, Rose-John S, Ludwig A. The disintegrin-like metalloproteinase ADAM10 is involved in constitutive cleavage of CX3CL1 (fractalkine) and regulates CX3CL1-mediated cell-cell adhesion. Blood. 2003; 102:1186–1195. [PubMed: 12714508]
50. Duffy MJ, McKiernan E, O'Donovan N, McGowan PM. Role of ADAMs in cancer formation and progression. Clin Cancer Res. 2009; 15:1140–1144. [PubMed: 19228719]
51. Edwards DR, Handsley MM, Pennington CJ. The ADAM metalloproteinases. Mol Aspects Med. 2008; 29:258–289. [PubMed: 18762209]
52. Leksa V, Loewe R, Binder B, Schiller HB, Eckerstorfer P, Forster F, Cardona AS, Ondrovicova G, Kutejova E, Steinhuber E, Breuss J, Drach J, Petzelbauer P, Binder BR, Stockinger H. Soluble M6P/IGF2R released by TACE controls angiogenesis via blocking plasminogen activation. Circ Res. 2011; 108:676–685. [PubMed: 21273553]
53. Andersson S, Davis DL, Dahlbäck H, Jornvall H, Russell DW. Cloning, structure, and expression of the mitochondrial cytochrome P-450 sterol 26-hydroxylase, a bile acid biosynthetic enzyme. J Biol Chem. 1989; 264:8222–8229. [PubMed: 2722778]
54. Oshima A, Nolan CM, Kyle JW, Grubb JH, Sly WS. The human cation-independent mannose 6-phosphate receptor. Cloning and sequence of the full-length cDNA and expression of functional receptor in COS cells. J Biol Chem. 1988; 263:2553–2562. [PubMed: 2963003]
55. Garmroudi F, Devi G, Slentz DH, Schaffer BS, MacDonald RG. Truncated forms of the insulin-like growth factor II (IGF-II)/mannose 6-phosphate receptor encompassing the IGF-II binding site:

characterization of a point mutation that abolishes IGF-II binding. Mol Endocrinol. 1996; 10:642–651. [PubMed: 8776724]

56. Pear WS, Nolan GP, Scott ML, Baltimore D. Production of high-titer helper-free retroviruses by transient transfection. Proc Natl Acad Sci USA. 1993; 90:8392–8396. [PubMed: 7690960]
57. Schaffer BS, Lin M-F, Byrd JC, Park JHY, MacDonald RG. Opposing roles for the insulin-like growth factor (IGF)-II and mannose 6-phosphate (Man-6-P) binding activities of the IGF-II/Man-6-P receptor in the growth of prostate cancer cells. Endocrinology. 2003; 144:955–966. [PubMed: 12586773]
58. Hossenlopp P, Seurin D, Segovia-Quinson B, Hardouin S, Binoux M. Analysis of serum insulin-like growth factor binding proteins using Western blotting: use of the method for titration of the binding proteins and competitive binding studies. Anal Biochem. 1986; 154:138–143. [PubMed: 2422981]
59. Hartman MA, Kreiling JL, Byrd JC, MacDonald RG. High-affinity ligand binding by wild-type/mutant heteromeric complexes of the mannose 6-phosphate/insulin-like growth factor II receptor. FEBS J. 2009; 27:1915–1919. [PubMed: 19236480]

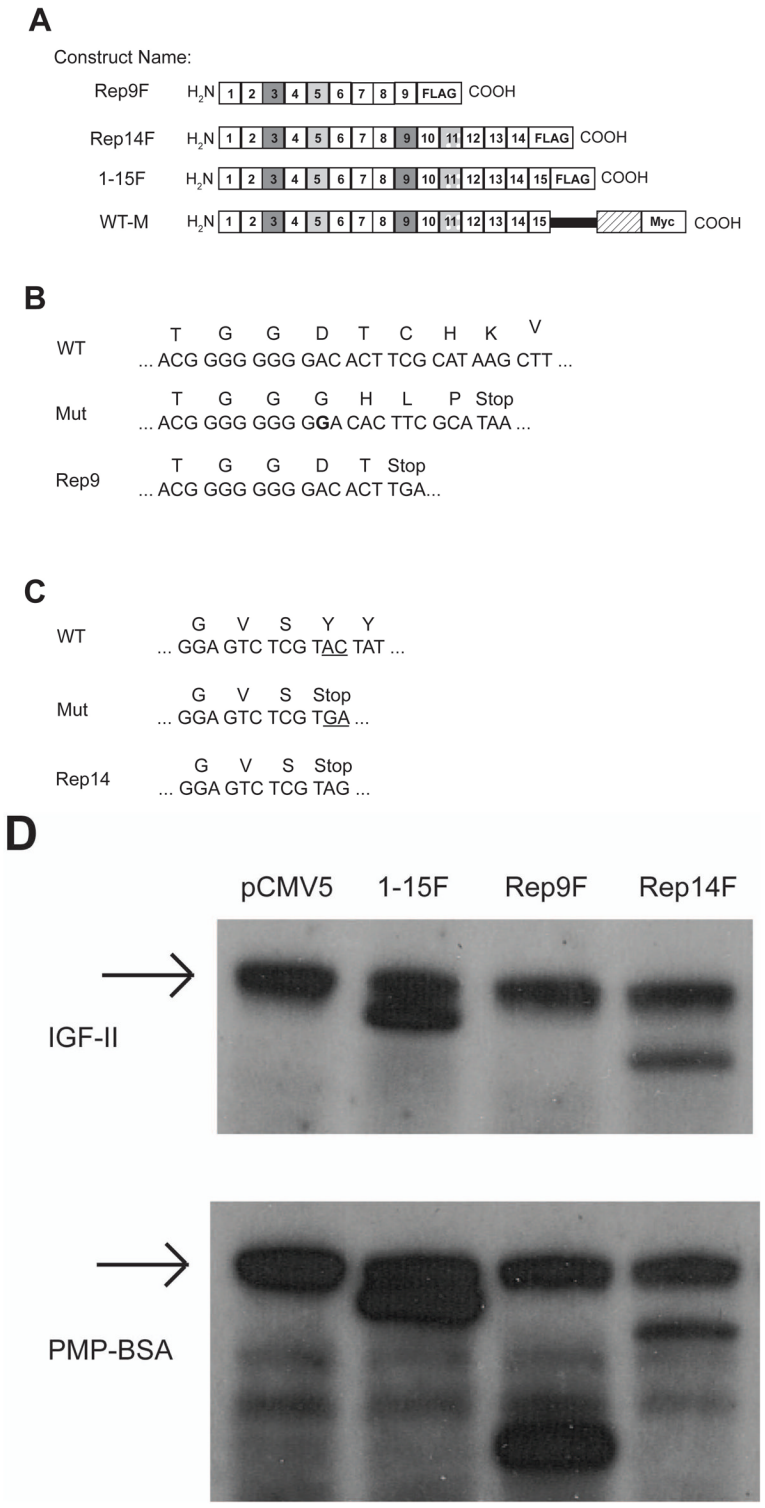

Figure 1. M6P/IGF2R Constructs and the Cancer-Associated Truncation Mutations

A, The receptor constructs are diagrammed with *squares* representing the repeating units (MRH domains) of the M6P/IGF2R ectodomain. The *dark gray boxes* represent the locations of the high-affinity M6P binding sites in repeats 3 and 9. The *light gray boxes*

represent the low-affinity M6P binding site in repeat 5, and the *stippled gray boxes* indicate the location of the principal IGF-II binding site in repeat 11. *Rectangles* denote the addition of the FLAG or Myc epitope tags to the C-termini of the proteins. The *solid black bar* represents the transmembrane domain of the full-length M6P/IGF2R, and the *hatched rectangle* indicates the M6P/IGF2R cytoplasmic region. *B and C,* Oligonucleotides were prepared to amplify the indicated regions of the human M6P/IGF2R cDNA sequence, thereby creating termination codons that mimic the truncations resulting from naturally occurring mutants (*Mut*). *B)* Insertion of a G (*bolded*) within the poly-G tract causes a frameshift in the mutant, leading to an early termination codon. *C)* A C:G to A:T transversion downstream of the region shown in *M6P/IGF2R* exon 40 creates a novel splice site that leads to premature termination after Ser^{2023}. *D)* Ligand blots of lysates (50 μg protein per lane) from cells transfected with cDNAs encoding the various truncated M6P/IGF2R species. Blots were probed with ^{125}I-IGF-II (top panel) or ^{125}I-PMP-BSA (bottom panel). The *arrow* indicates ligand binding to the endogenous M6P/IGF2R.

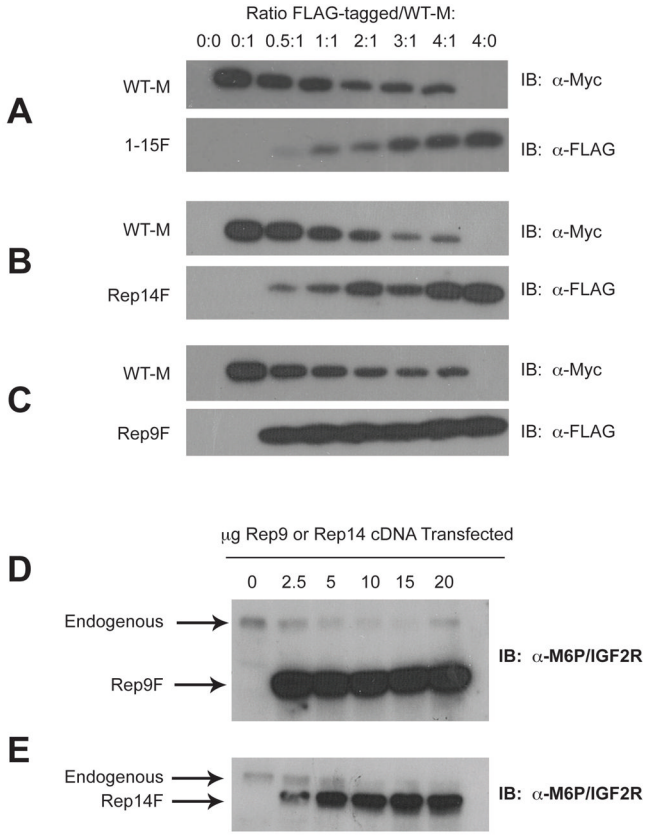

Figure 2. Transient Expression of M6P/IGF2R Constructs in HEK 293 Cells

HEK 293 cells were transfected or co-transfected with the indicated ratios of the FLAG-tagged truncated M6P/IGF2R vs. WT-M cDNA constructs. Total DNA transfected was adjusted to 25 μg per 100-mm dish by balancing with vector DNA. Aliquots (25 μL) of detergent extracts were resolved by SDS-PAGE on 6% gels, immunoblotted with α-FLAG, α-Myc, or α-M6P/IGF2R antibodies, and developed by autoradiography. A blot representative of at least three transfections is shown as follows: co-transfection of WT-M with *A)* 1–15F; *B)* Rep14F; or *C)* Rep9F, or single transfection of the indicated amounts of *D)* Rep9F or *E)* Rep14F. Arrows in *parts D and E* represent expression of the indicated constructs. Regression analysis indicated that the effects of truncated receptor on expression of the full-length receptors were significant: *A*) $P < 0.0001$; *B*) $P < 0.003$; *C*) $P < 0.0002$; *D*) $P < 0.015$: *E*) $P < 0.004$.

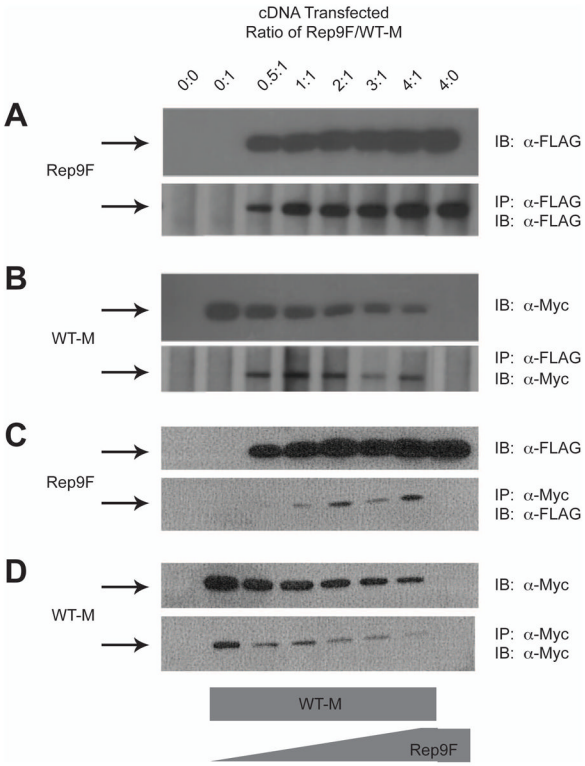

Figure 3. Co-immunoprecipitation of Rep9F and WT-M Receptors from Co-transfected HEK 293 Cells

The ability of WT-M to co-immunoprecipitate with Rep9F was measured by immunoprecipitation assays. *A,B:* Immunoprecipitation with α-FLAG affinity resin: Equal protein (100 μg) of Triton X-100 extracts from HEK 293 cells co-transfected with increasing Rep9F (0–20μg) and a constant amount of WT-M (5 μg) cDNA were immunoprecipitated with 8 μl of α-FLAG resin in a volume of 0.2 mL. The resin pellets were collected by centrifugation, washed, and heated in sample buffer with DTT. The proteins from the resin pellets (lower panels) and additional samples of lysates that were not immunoprecipitated (upper panels) were resolved bySDS-PAGE on 6% gels, subjected to immunoblot analysis with α-FLAG (*panel A*) or α-Myc (*B*) antibodies, and developed by autoradiography. Representative blots are shown. *C,D:*α-Myc immunoprecipitation and subsequent immunoblot analysis of Rep9F and WT-M. Equal volumes (20 μl) of detergent extracts from co-transfected HEK 293 cells were incubated with 1 ml of α-Myc antibody in a volume of 0.1 mL. Subsequently, aliquots (25 μl) of washed/blocked Protein G-Sepharose were added to the reactions in a total volume of 0.2 mL and incubated further for immunoprecipitation. The pellets were processed and analyzed as in *A and B, respectively*. The blots shown are representative of 3 replicate experiments.

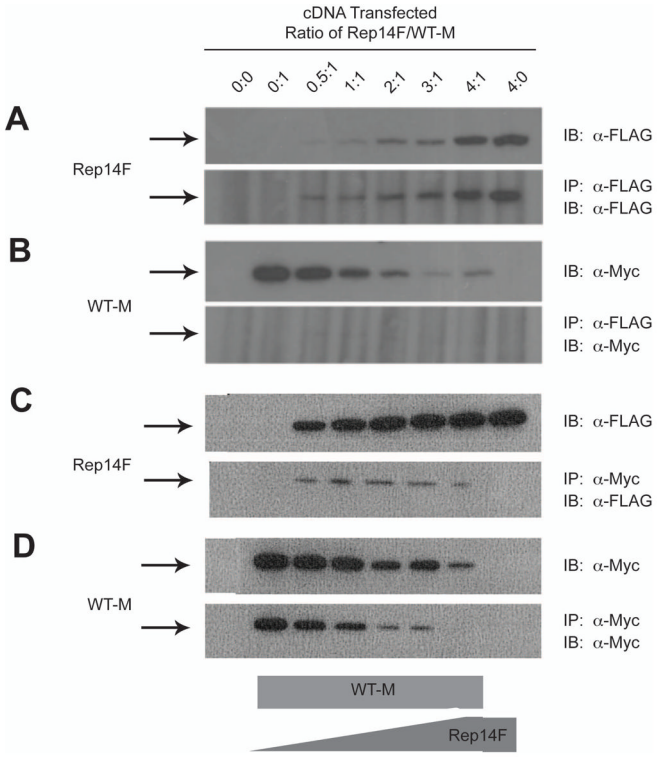

Figure 4. Co-immunoprecipitation of Rep14F and WT-M Receptors from Co-transfected HEK 293 Cells

The ability of WT-M to co-immunoprecipitate with Rep14F was measured by immunoprecipitation assays as in Figure 3. *A,B:* Immunoprecipitation with α-FLAG affinity resin followed by blotting with α-FLAG (*A*) or α-Myc (*B*) antibodies. *C,D:*α-Myc immunoprecipitation and subsequent immunoblot analysis of Rep14F and WT-M. The blots shown are representative of 3 replicate experiments.

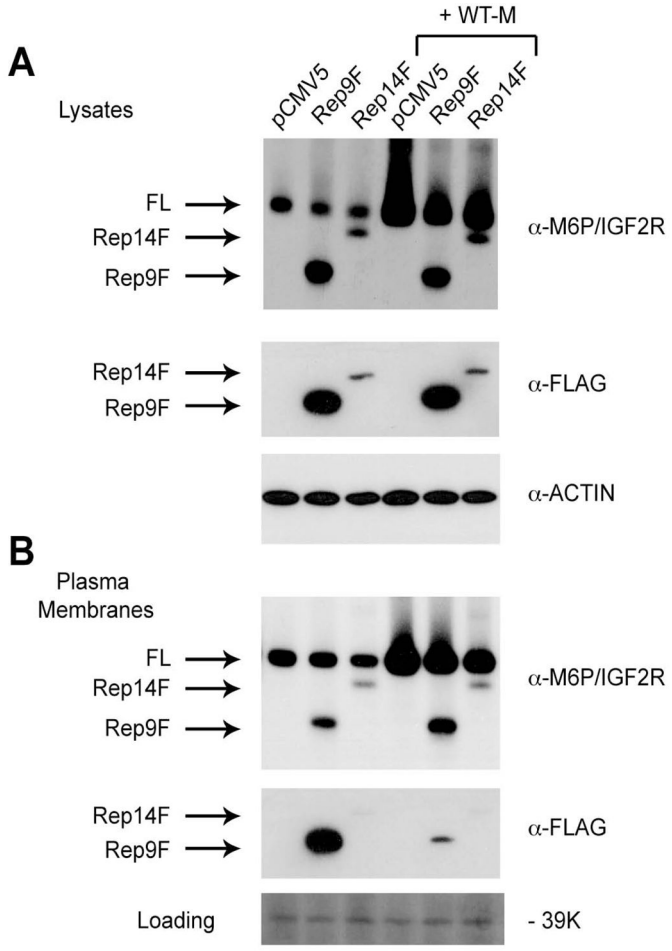

Figure 5. Effect of Truncated Receptor Expression on the Amount of Full-Length M6P/IGF2R in Whole-Cell Lysates vs. Plasma Membranes

HEK 293 cells were transfected with pCMV5 vector or the cDNAs (10 μg) encoding Rep9F or Rep14 alone or by co-transfection with empty vector or 10 μg of cDNA encoding the full-length WT-M receptor, as indicated. Transfected DNA was balanced to a total of 20 μg per dish in all cases. Aliquots (50μg protein) of *A)* detergent extracts (lysates) and *B)* plasma membranes were analyzed by immunoblotting with the antibodies indicated to the right of each panel. Arrows designate the various forms of the receptor. *B, bottom panel* shows a portion of the plasma membrane blot stained with a solution of 0.1% Ponceau S in HBS; the intensity of an irrelevant 39K band serves as a loading control. One-way ANOVA of the data from three replicate experiments indicated that differences in intensity of the full-length bands were not significant when comparing Rep9F-transfected vs. pCMV5 vector or Rep9F co-transfected with WT-M controls. The effect of Rep14F on intensity of the endogenous receptor bands and the WT-M exogenous receptor bands was significant ($P < 0.025$) in both lysates and plasma membranes.

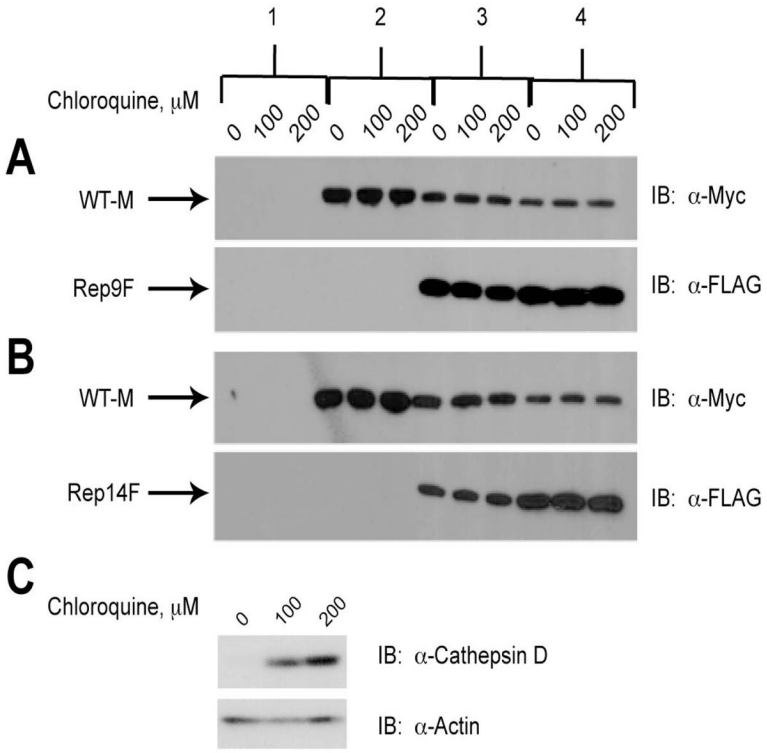

Figure 6. Lack of Effect of Chloroquine on Degradation of Wild-type M6P/IGF2R in Response to Co-expression with Truncated Constructs

HEK 293 cells were transfected with the cDNA constructs as indicated along the top of the panel: 1) 25 μg pCMV5 vector control; 2) 5 μg WT-M cDNA; 3) 5 μg WT-M + 5 μg mini-receptor cDNAs; 4) 5 μg WT-M + 15 μg mini-receptor cDNAs. Vector control DNA was also added in samples 2 and 3 to normalized DNA transfected to 25 μg per dish. Twenty-four hours after transfection, the cells were treated with the indicated concentrations of chloroquine for 16 h to inhibit lysosome-based protein degradation. Detergent extracts were prepared and 100 μg of total protein from each lysate condition was resolved by SDS-PAGE on 6% gels, immunoblotted with α-FLAG or α-Myc antibodies, and developed by autoradiography. *Arrows* represent the various forms of the M6P/IGF2R expressed in HEK 293 cells. Blots shown are representative of three transfections as follows: co-transfection of *A*) WT-M and Rep9F; *B*) WT-M and Rep14F. *C*) Positive control showing the effect of chloroquine on expression of cathepsin D (α-cathepsin D antibody at 1:500 dilution). Within each transfection group, there was no significant effect of chloroquine on the intensities of the WT-M bands: *A* and *B*) $P > 0.05$ in all comparisons.

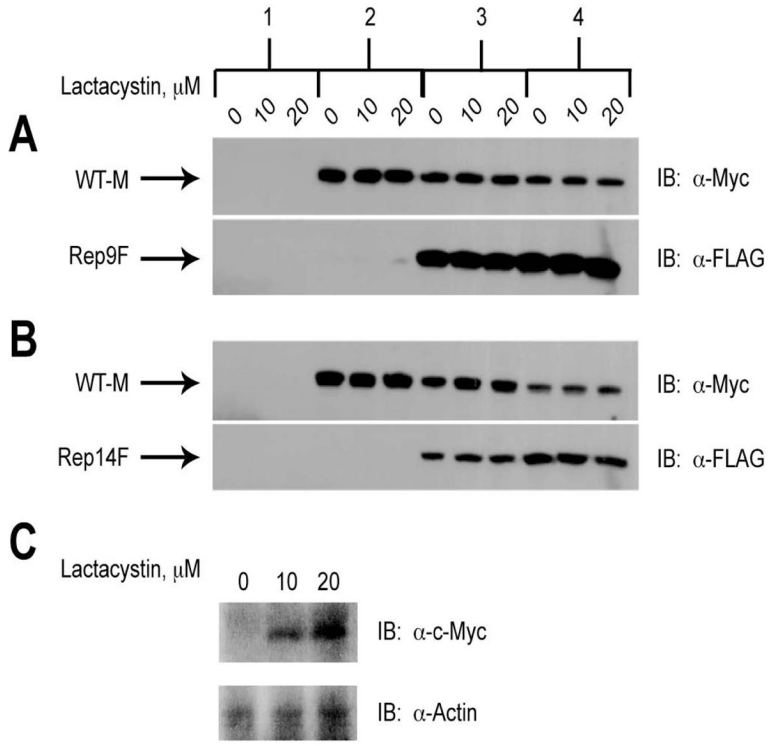

Figure 7. Lack of Effect of Lactacystin on Degradation of Wild-type M6P/IGF2R in Response to Co-expression with Truncated Constructs

HEK 293 cells were transfected with the cDNA constructs as indicated along the top of the panel: 1) 25 μg pCMV5 vector control; 2) 5 μg WT-M cDNA; 3) 5 μg WT-M + 5 μg mini-receptor cDNAs; 4) 5 μg WT-M + 15 μg mini-receptor cDNAs. Vector control DNA was also added in samples 2 and 3 to normalized DNA transfected to 25 μg per dish. Twenty-four hours after transfection, the cells were treated with the indicated concentrations of lactacystin for 16 h to inhibit proteasomal activity. Detergent extracts were prepared and 100 μg of total protein from each lysate condition was resolved by SDS-PAGE on 6% gels, immunoblotted with α-FLAG or α-Myc antibodies, and developed by autoradiography. *Arrows* represent the various forms of the M6P/IGF2R expressed in HEK 293 cells. Blots shown are representative of three transfections as follows: co-transfection of *A*) WT-M and Rep9F or *B*) WT-M and Rep14F. *C*) Positive control showing the effect of lactacystin on expression of c-Myc (α-Myc antibody at 1:500). Within each transfection group, there was no significant effect of lactacystin on the intensities of the WT-M bands: *A* and *B*) $P > 0.05$ in all comparisons.

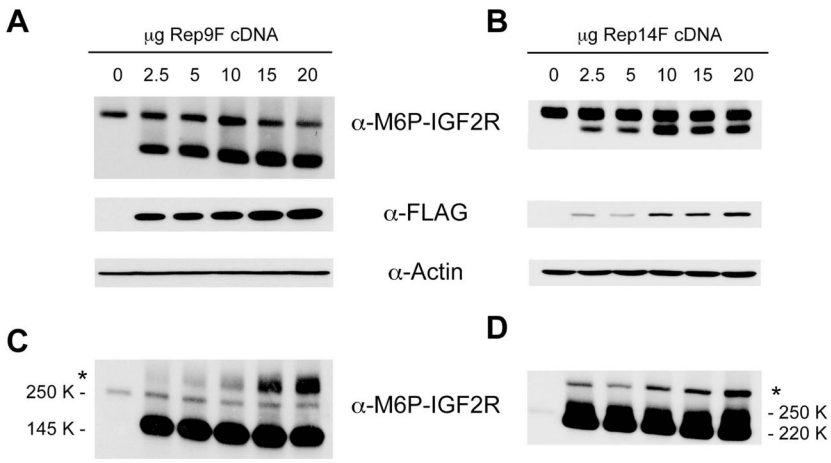

Figure 8. Proteolytic Cleavage of Cell-Surface M6P/IGF2R is Increased in the Presence of Truncated Receptors

Detergent extracts (*Panels A and B*, 100 μg protein) or concentrated conditioned medium (CCM, *Panels C and D*, 50 μl volume) from HEK 293 cells transfected with the indicated amounts of the Rep9F or Rep14F cDNA constructs were resolved by SDS-PAGE on 6% gels, immunoblotted with the indicated antibodies, and developed by autoradiography. Blots representative of at least three transfections are shown as follows: *A,C)* Rep9F and *B,D)* Rep14F. The *asterisks* in *Panels C and D* indicate the presence of a high-molecular-weight complex of containing M6P/IGF2R but of unknown composition... Regression analysis indicated that the effects of the Rep9F truncated receptor on expression of the full-length receptor in lysates (*A, left panel, P* <0.03) and the amount of M6P/IGF2R ectodomain shed into CCM (*B, left panel, P* <0.0002) were significant. The effect of the Rep14F truncated receptor on expression of the full-length receptor in lysates (*A, right panel*) was significant (*P* <0.02), but the band intensities for the ectodomain in CCM (*B, right panel*) could not be quantified due to lack of resolution from the Rep14F band.

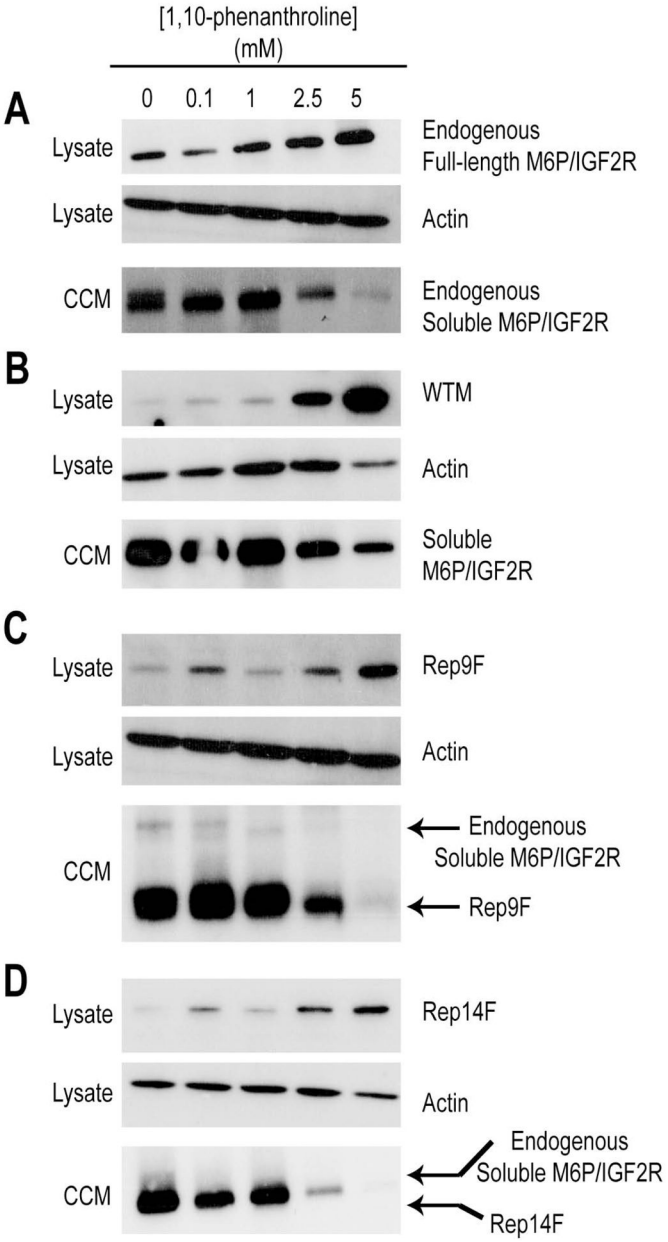

Figure 9. Inhibition of M6P/IGF2R Ectodomain Shedding by 1,10-Phenanthroline

HEK 293 cells were transfected with empty pCMV5 vector (25 μg DNA) (*A*) or with the cDNA constructs indicated along the right side of each panel: *B*) 25 μg WT-M cDNA; *C*) 25 μg Rep9F cDNA; or *D*) 25 μg Ref14F cDNA. On the day after transfection, the cells were switched to serum-free medium plus the indicated concentrations of 1,10-phenanthroline. On the third day after transfection, 48-h concentrated conditioned medium (CCM) and whole-cell lysates were prepared. Aliquots (100 μg protein) of the lysates and CCM (50 μl volume) were analyzed by immunoblotting with the antibodies indicated to the right of each panel. The blots for actin as loading control apply to lysate samples only. These data are representative of three replicate experiments. Regression analysis indicated that the effects of OPA treatment on retention of the various receptor species in lysates were significant: *A*) $P < 0.005$; *B*) $P < 0.02$; *C*) $P < 0.006$; *D*) $P < 0.005$.